# A Robot with an Augmented-Reality Display for Functional Capacity Evaluation and Rehabilitation of Injured Workers

Jason Fong[1], Renz Ocampo[1], Douglas P. Gross[2], and Mahdi Tavakoli[1]

***Abstract*— Occupational rehabilitation is an integral part of the recovery process for workers who have sustained injuries at the workplace. It often requires the injured worker to engage in functional tasks that simulate the workplace environment to help regain their functional capabilities and allow for a return to employment. We present a system comprised of a robotic arm for recreating the physical dynamics of functional tasks and a 3D Augmented Reality (AR) display for immersive visualization of the tasks. While this system can be used to simulate a multitude of occupational tasks, we focus on one specific functional task. Participants perform a virtual version of the task using the robot-AR system, and a physical version of the same task without the system. This study shows the results for two able-bodied users to determine if the robot-AR system produces upper-limb movements similar to the real-life equivalent task. The similarity between relative joint positions, i.e., hand-to-elbow (H2E) and elbow-to-shoulder (E2S) displacements, is evaluated within clusters based on the spatial position of the user's hand. The H2E displacements for approximately 50% of hand position clusters were consistent between the robot-AR and real-world conditions and approximately 30% for E2S displacements. The similar clusters are distributed across the entire task space however, indicating the robot-AR system has the potential to properly simulate real-world equivalent tasks.**

## I. Introduction

The growing demand for rehabilitation services following a workplace injury has motivated the development of new technologies for robotics-assisted assessment and rehabilitation of motor function following injury. The standard practice in occupational (or vocational) rehabilitation is to first perform a functional assessment of the injured worker. Typically, this is done using a Functional Capacity Evaluation (FCE) that assesses a worker's performance in a set of standard tasks [1], where each task requires different sets of equipment. The tasks incorporated in the FCE may involve material-handling activities such as lifting, pushing, and pulling, and positional tolerance activities such as walking, reaching, and grasping.

The first problem with the above is that it needs a large amount of equipment for various functional tasks and the space to store them. While a small number of all-in-one computer-based assessment tools exist [2], [3], they are highly specialized in design and can replicate only specific rehabilitation tasks. A second problem emerges due to the current standardized assessments, where therapists qualitatively assess a patient's performance based on what they can observe. More complex, quantitative and objective assessments are desired. A third problem occurs when therapists increase the difficulty of a task or ask the injured workers to execute tasks that are considered boring; the patients can become bored, unmotivated, or uncooperative.

To address the above issues, we propose a generalized robotics-based solution. Our solution incorporates a serial-manipulator and a projection-based Augmented Reality (AR) display in order to provide a unified tool for both FCE and rehabilitation that is immersive and device-independent. To evaluate the efficacy of the proposed system, the biomechanics of the user's arm while using the system is retrieved and compared against the biomechanics of their arm in an equivalent real-life performance of the same task. In this regard, we present the following hypothesis: The proposed system can be used as an alternative to traditional occupational rehabilitation exercise environments because *it does not significantly modify the biomechanics of the user's arm while performing functional tasks compared to the conventional task performance.*

The paper is structured as follows: Section II is a brief overview of the work found in the literature that relates to our proposed approach. Section III describes the design of the rehabilitation exercise and experimental procedure. Section IV presents the results and provides a discussion based on the performed data analysis. Finally, Section V concludes the findings and examines possible directions for future work.

## II. Related Work

### A. FCE

FCE is widely used to assess injured workers before, during and after rehabilitation. A number of studies have demonstrated the reliability and validity of FCE and correlation with future recovery and return to work. Peppers et al. showed that augmenting clinical evaluation with FCE improves physicians' assessments of the patient's skills and work capacities [4]. Gross et al. studied the impact and benefits of integrating FCE into rehabilitation for better outcomes for injured workers [5]. FCE has been found to significantly predict return to work [6] and is an integral component of graded activity and functional rehabilitation programs [7]. However, James et al. concluded that further

This research was supported by the Canada Foundation for Innovation (CFI) under grant LOF 28241; the Alberta Innovation and Advanced Education Ministry under Small Equipment Grant RCP-12-021; the Natural Sciences and Engineering Research Council (NSERC) of Canada under the Collaborative Health Research Projects (CHRP) Grant #316170; and Quanser, Inc.

[1]J. Fong, R. Ocampo and M. Tavakoli are with the Department of Electrical and Computer Engineering, University of Alberta, Edmonton, Canada (email:jmfong@ualberta.ca, rocampo@ualberta.ca, mahdi.tavakoli@ualberta.ca)

[2]D. Gross is with the Faculty of Rehabilitation Medicine, University of Alberta, Edmonton, Canada (email:doug.gross@ualberta.ca)

research is needed in FCE, especially on the use of computer technology (including robotics and digital sensors) [8].

### B. Robot-assisted Assessment Rehabilitation

The inclusion of robots in therapy is becoming more common thanks to robots' power, repetitive motion ability, reprogramming capacity and potential adaptability to new tasks. These features allow robots to be used in therapy fields such as emotional therapy and physical therapy. Yakub et al. provide a list of robots developed in the context of rehabilitation medicine [9]. The use of robots in occupational rehabilitation began in the early 1990s [10], [11], although they were employed mainly as assistive devices for workers with injury or disability. Recent developments in the area have culminated in devices such as BTE's EvalTech [2] and Simwork's Ergos II [3] systems, which simulate FCE assessment setups and can also be used for strength and movement coordination training. However, these devices are specifically designed to emulate a certain set of FCE tasks. Also, the performance of tasks with these systems are spatially constrained to their placement on the devices and the performance of tasks involving free-space motions is not an option. For instance, while a device may include a lock for practicing turning a key to open it, the more challenging task for painting a wall is not supported because it cannot be done at one point on the device. The tasks also remain limited by the need to have physical objects that the user holds during assessments (e.g., rotating handles and knobs).

### C. Virtual Reality & Augmented Reality in Rehabilitation

Virtual reality (VR) and AR technology has been making its way into the rehabilitation field in recent years. It has been shown to increase the motivation of patients and keep them engaged since it uses games to disguise the repetitive movements of the rehabilitation exercises [12]. However, most of the VR and AR rehabilitation systems in the literature and on the market are targeted for those who have been affected by neurological injuries due to events such as stroke and spinal cord injury [13]. These systems cannot be used by injured workers as-is due to the difference in challenge level and sophistication of the rehabilitation tasks between the two groups (i.e., stroke patients and injured workers).

For non-immersive VR, in which the game is displayed in a 2D screen in front of the patient, there exist systems like the BTE Eccentron [14] to improve lower-limb strength while providing an interactive game-like experience to guide the patient toward their objectives. To the best of the authors' knowledge, there are currently no immersive VR or AR systems that train injured workers to regain muscle strength to enable them to return to work. There is also no robotic system that is specifically developed for simulating the physical dynamics of functional tasks for the rehabilitation of injured workers. Our proposed system employs the use of a 3D spatial AR display to immerse the patient in a projected 3D virtual environment that is integrated with the physical environment including the robotic manipulator. Previous research from our group shows that the resultant colocation of visual and motor axes help improve user performance in rehabilitation exercises [15].

We propose an approach based on using a seven Degree-of-Freedom (DoF) serial manipulator for simulating the physical dynamics (i.e., haptic interaction) corresponding to functional tasks, eliminating the need for physical hardware of such tasks. Compared to rehabilitation facilities that allocate a large area for multiple tasks, this unified system can reduce the costs for equipment. Our approach also integrates an AR display to provide reconstructed visual feedback of the simulated task in an immersive environment. All types of motions can be performed on the robot due to its seven DoF design. This allows flexibility in movement that is not found in other systems. Furthermore, having a robotic system allows for masking the task parameters from the patient which can help prevent the loss of motivation from knowing about an increase in the difficulty level of the task.

The overall robot-AR system is useful for both FCE and rehabilitation of injured workers. Serial manipulators have been previously incorporated into rehabilitation medicine for both assessment and rehabilitation purposes [16]. Our group, in particular, has extensively applied serial rehabilitation robots to target the neuromuscular rehabilitation of patients with stroke [17], [18]. Likewise, we have also developed a robot-assisted AR system for simulated stroke patients, in which the effects of stroke (e.g., being distracted) is simulated by cognitively loading the user with a count down task. However, to the best of our knowledge, the use of robots and AR in the context of facilitating FCE and rehabilitation of injured workers remains unexplored.

## III. Materials and Methods

### A. Rehabilitation Task Design

The simplified movements found in rehabilitation tasks often involve reaching, grasping, and weight lifting. The task used in our robot-AR system implements these movements in their basic forms but can be further adapted to higher difficulty and complexity levels.

We chose a painting task that trains up-down hand movements by having the user paint a vertical wall. A fill indicator provides the user with information on the percentage of the wall that is already painted. Force feedback is provided by the robot when the virtual paint roller is in contact with the wall so that the haptic experience of painting on the wall in the real world is recreated. In the real-world condition, the user is given a physical paint roller to use on a portable physical wall positioned at the same spot the virtual wall was in the robot-AR condition. No paint is used in the real case; rather, the user is asked to "paint over" an area of the wall as much as they can. The user "paints" until the area they have covered encompasses the wall in the virtual task. Measurements such as time of completion and amount of force exerted by the user can potentially be retrieved and analyzed in the robot-AR setup, but are not within the focus of this paper.

### B. Robotic Manipulator Choice and Control Strategy

Many standardized FCEs such as the WorkWell FCE and the Progressive Isoinertial Lifting Evaluation (PILE) place emphasis on an injured worker's ability to lift weighted objects (e.g., crates) as an important assessment, among other physically strenuous tasks [1]. Therefore, it is desirable to use a robot capable of exerting enough force to realistically simulate heavy objects and interactions with environments typical of an injured worker's workplace. For this reason, the robot used in this work is a heavy-duty industrial robot; details are provided in Section III-C. Internal gearing makes the structure of the robot non-back-drivable; however, the requirement of physical human-robot interaction (PHRI) in our experiments means a suitable robotic controller is needed to make the robot back-drivable.

Impedance controllers, which output a force for a robot to exert based on its motion, are ideal for providing stable PHRI when simulating environmental interactions. However, implementing such controllers typically requires full knowledge of the robot's dynamics parameters such as each joint's mass and center of mass [19], which are unavailable for the robot used in this work and difficult to accurately measure. Admittance controllers, which output a motion for the robot to execute based on a measured force input, are a common alternative for non-back-drivable, heavy-duty robots like the one used in this paper. The general form of an admittance controller's transfer function is

$$G = \frac{\vec{V}_d\left(s\right)}{\vec{W}\left(s\right)} = \frac{1}{Ms + B} \tag{1}$$

Note that in this paper, an internal velocity controller is used by the robot to perform movements in real-time, so the admittance controller is designed here to output a desired velocity rather than a desired position. The input to the controller, $\vec{W}\left(s\right) = \left[\vec{F}\left(s\right), \vec{\tau}\left(s\right)\right]^{\intercal}$, represents the wrench composed of input forces and torques, and the output, $\vec{V}_d\left(s\right)$, is the resulting desired velocity, composed of Cartesian and angular terms. $M$ represents the desired mass and inertia matrix and $B$ represents the desired Cartesian and angular damping matrix. These matrices affect the transparency of free motion experienced by the user and also the stability of the robot. A stiffness parameter is not used, similar to [20], because restoring forces are not desirable during co-manipulation in free-space. It follows that $G$ is given as

$$G = \begin{bmatrix} g_x & 0 & 0 & 0 & 0 & 0 \\ 0 & g_y & 0 & 0 & 0 & 0 \\ 0 & 0 & g_z & 0 & 0 & 0 \\ 0 & 0 & 0 & g_\alpha & 0 & 0 \\ 0 & 0 & 0 & 0 & g_\beta & 0 \\ 0 & 0 & 0 & 0 & 0 & g_\gamma \end{bmatrix}$$

where $\{g_x,\ g_y,\ \ldots,\ g_\gamma\}$ represent the admittance terms for each Cartesian direction and orientation angle. Large values for admittance terms result in greater allowed motions while small values result in more constrained movements. By changing the admittance parameters, allowed movements initiated by the user can be restricted to certain axes. This is used, for example, in our task where it is beneficial to restrict rotations in axes that are not of interest (e.g., small values for $g_\beta$ and $g_\gamma$) while allowing free motion in the other axes (e.g., large values for $g_x$, $g_y$, $g_z$, and $g_\alpha$).

### C. Experimental Setup

As seen in Fig.1, the robot-AR system uses a Motoman SIA-5F (Yaskawa America, Inc., Miamisburg, Ohio, USA) seven DoF serial manipulator as the user interface to control the paint roller in the virtual environment. It is controlled using MATLAB, Simulink, and C++ in which the flow of communication between them is described in [21]. Attached to the robot's wrist joint before the end-effector is a 6-DoF ATI Gamma Net force/torque sensor (ATI Industrial Automation, Inc., Apex, North Carolina, USA). The AR subsystem consists of an off-the-shelf InFocus IN116A projector mounted 3 $m$ above the ground that projects to a screen on the table. A Microsoft Kinect V2 Sensor is positioned 1.2 $m$ horizontally distant and 0.34 $m$ vertically above the user's head to enable head tracking for displaying the correct perspective to the user. To properly view the 3D scene, active DLP-Link 3D shutter glasses are worn by the user. The development of the 3D environment is done using the Unity Game Engine [22] where a virtual model of the workspace is created. This virtual model is created and calibrated to the world scale using Microsoft's RoomAlive Toolkit [23]. A ClaroNav MicronTracker (ClaroNav, Inc., Toronto, Ontario, Canada) motion tracking camera (MTC) is used to record the positions of the user's hand, elbow, and shoulder.

As mentioned earlier, the requirements of the more strenuous FCE and rehabilitation tasks imply a need for high force and torque haptic interactions. The admittance-type Motoman robot is used as the manipulator due to its heavy load capabilities compared to other impedance-type haptic interfaces. It has a payload limit of 5 $kg$ for accurate movement and can generate joint torques up to a rated 300 $Nm$. These are the maximum values achievable by the robot and we do not use all of it. For safety, constraints are placed in the software to limit high velocities and position singularities. The attached force sensor records user force and torque inputs, which are used to facilitate the admittance control of the robot.

The painting task requires a specific setup of the projector around the robot due to the limited projection space and required robot configuration. The configuration uses a curved screen with dimensions 85 $cm$ tall, 75 $cm$ deep, and 56 $cm$ wide situated on top of the table. The end-effector of the robot is positioned to the right of the screen. This configuration allows the user to have an intuitive feel of the simulated task and reduces the occlusions on the projection display caused by the user's arm and robot joints.

### D. Experimental Procedure

5 trials for each condition (i.e., robot-AR or real-world) are carried out to have a total of 10 trials per person, lasting approximately 60 $s$ per trial. The trials are performed by

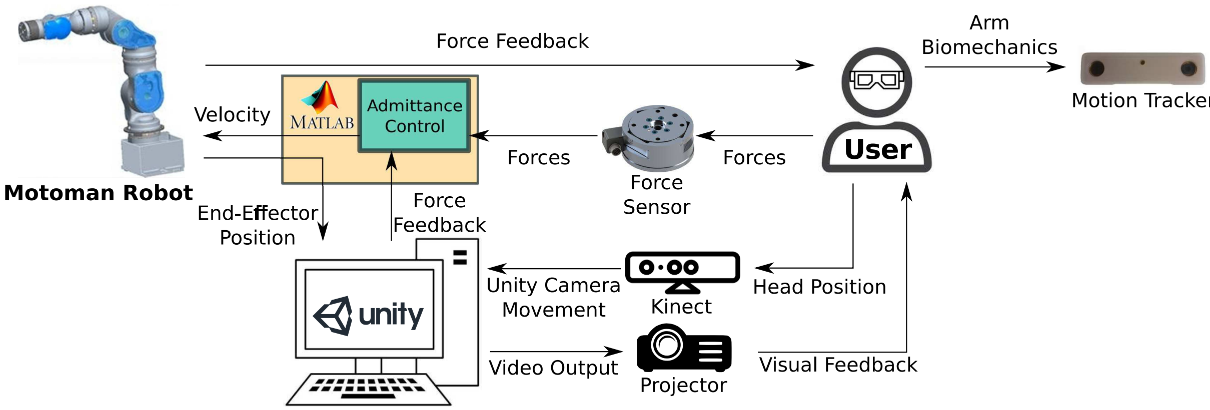


Fig. 1. Flowchart of the communication between each system.

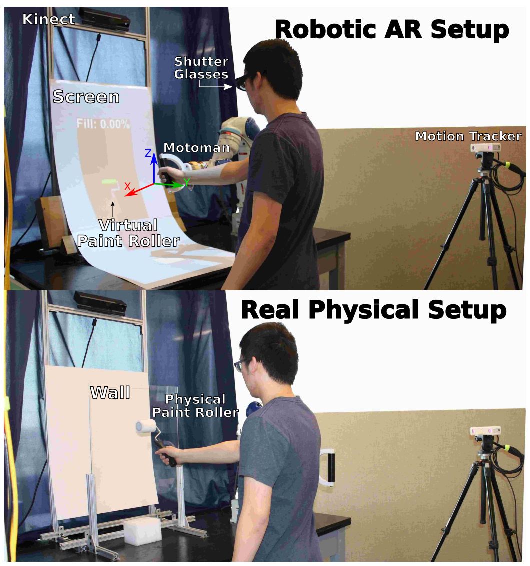


Fig. 2. Painting task experimental setup for the robot-AR condition (top) and the real-life equivalent condition (bottom). The projector is not shown. Through AR, the paint roller will pop out in 3D from the perspective of the user in a geometrically correct position and orientation relative to the robot end-effector.

2 able-bodied participants (both are male, 24 years old, and right-handed). Each participant is asked to stand in a comfortable position in front of the screen and to hold the Motoman robot's end-effector with his arm half extended. The participant is instructed to refrain from changing his standing location, which is marked on the floor, between the two experimental conditions. A chair is provided for the participant to take rests when needed. All 5 trials are recorded for a specific condition before moving onto the other one. The robot-AR condition for the painting task is presented to *Participant 1* as the first set of trials before doing the trials under the real-world condition. The opposite order is presented to *Participant 2*.

## IV. Results and Discussion

The hand, elbow, and shoulder positions recorded by the MTC form the data for the biomechanics analysis performed. These are recorded by placing fiducial markers on the back of the user's hand, and on the elbow and shoulder. To evaluate the similarity of the biomechanics between using the proposed system and the equivalent real-world task, we consider the hand position as the independent variable and the elbow and shoulder positions as the dependent variables. In other words, while the user's hand position changes, the elbow and shoulder joint positions will change in order to best accommodate the desired hand pose. For a fixed hand position (independent variable), we will compare the distribution of the dependent variables between the two conditions.

The two-sample Kolmogorov-Smirnov (KS) test is a commonly used method of evaluating whether two one-dimensional distributions are statistically different (the null hypothesis is that they are similar). Since $p_{H-E}$ and $p_{E-S}$ are in three dimensions, we use the modified version of the KS test in three dimensions as described in [24] by Fasano and Franceschini. We make use of the implementation of Fasano and Franceschini's work in [25] in conjunction with the Monte-Carlo simulations provided in the original work.

A preliminary comparison between the datasets for the two conditions is performed first to see if the distribution of elbow and shoulder joint positions for the same hand position as it traverses the entire surface of the wall being painted is statistically similar between the two conditions. Here, the joint position data from the real-world condition is taken as the baseline data; for a specific hand position, the elbow and shoulder positions for the robot-AR condition should resemble those measured in the real-world condition. If this happens, it can be concluded that the robot-AR system does not significantly modify how users perform the task compared to the real-world condition. The process of comparison is given as follows: for each recorded hand position in the robot-AR dataset, a similar hand position in the real-world data is found by using a nearest-neighbor (NN) search. For these similar hand positions, the associated hand-to-elbow (H2E) and elbow-to-shoulder (E2S) displacements can be calculated in each dataset. The result is a distribution of H2E and E2S displacements recorded in the robot-AR condition, and a distribution of H2E and E2S displacements that are associated with the real-world condition for the

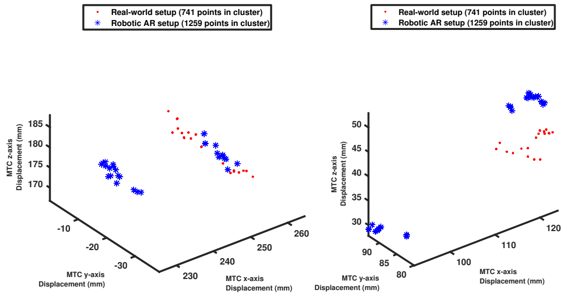


(a) (b)

Fig. 3. Joint position data for an example cluster. (a) shows the point cloud data for H2E displacements, and (b) shows E2S displacements.

same hand positions. The modified KS test is then used to compare the H2E displacement distributions, and the E2S displacement distributions between the two conditions. Note that [24] only provides Monte Carlo simulations up to a maximum $n = 500$, where in a two sample KS test $n = \frac{n_1 n_2}{n_1 + n_2}$ where $n_1$ and $n_2$ are the number of points in the real-world condition and robot-AR condition, respectively. Knowing that the number of points in the distributions is the same, i.e., $n_1 = n_2$, we then restrict the number of points in the distributions to 1000 points or less. To do this, the collection of datapoints are downsampled to 1000 points for each condition, resulting in 200 points per trial. A significance value is returned by the test and is compared against an alpha value of $\alpha = 0.05$.

The results for the H2E and E2S comparisons produced a value of $p < 0.05$, indicating that the distributions are statistically different (i.e., rejecting the null hypothesis that two conditions have the same distribution) and therefore suggests that the biomechanics of the two conditions are different. This motivates a closer inspection of the data.

Examining whether there are spatial trends in the similarity between the distributions may help explain the dissimilarity reported in the KS test for the full dataset. To do this, we propose to divide the data into spatial sections or voxels and performing the KS test for each voxel, looking for any that may be dissimilar. A grid of measurement points is first constructed by choosing points at evenly-spaced intervals to encompass the range of hand positions across all datasets in the three Cartesian dimensions. All recorded hand positions are then clustered to the nearest grid point using the NN search. We use an interval of 25 $mm$ as the distance between grid points, as it provides a high resolution of voxels in our task space and allows most clusters to meet the requirements for $n_1$ and $n_2$. Fig. 3 shows the distributions of H2E displacements and E2S displacements for an example cluster.

For each cluster, the statistical similarity of the distributions for the associated data from the two conditions (robot-AR and real-world setups) is then evaluated with the modified KS test. Similar to before, the Monte Carlo simulations in [24] are only provided for a minimum of $n = 10$ between two samples (and a maximum of $n = 500$). To ensure $10 \leq n \leq 500$, we impose conservative limits where $n_1 \geq 20, n_2 \geq 20$ and $n_1 + n_2 \leq 2000$. Graphical

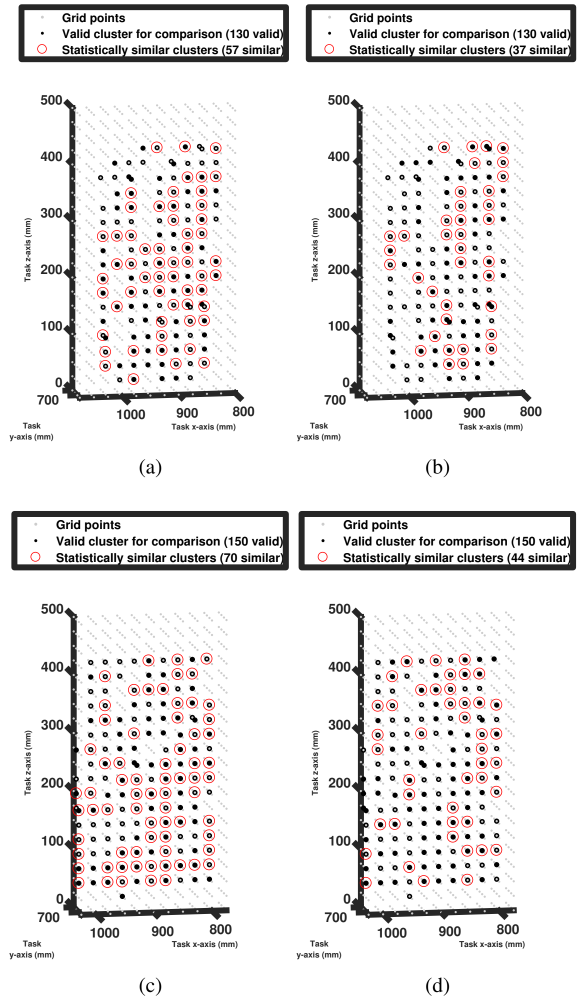


Fig. 4. Three-dimensional KS results for the painting task with the data split into voxels for comparison. The grid points show points in space around the surface of the wall where H2E and E2S results were clustered and compared at. (a) and (b) represent H2E and E2S results for *Participant 1*, respectively, and (c) and (d) represent the same for *Participant 2*. Clusters with a sufficient number of datapoints for comparison with the KS test are shown with black points and those of statistical similarity are circled in red.

results of the modified KS tests are shown in Fig. 4.

The percentage of clusters that are statistically similar between the two conditions show that 43.85% of the measurable clusters were similar for H2E displacements and 28.46% were similar for E2S displacements during Participant 1's trials. Participant 2 achieved 46.67% similarity for H2E displacements and 29.33% similarity for E2S displacements.

At first glance, the fraction of clusters that produced similar results seems to be quite low, especially for the E2S displacements. However, a qualitative observation of the results in Fig. 4 shows that the statistically similar clusters are well spread across the entire workspace. There are a few possible reasons as to why some clusters may not show similar results. As the real-world condition experiments did not involve actual paint being laid on the physical wall, keeping track of the "painted" portion proved to be challenging. This could affect the fairness of the KS test performed. For example, if, for a specific cluster, $n_1 \gg n_2$, where $n_1, n_2 > 20$, then a comparison of the distributions would be valid according to the restrictions we placed on the comparison in a cluster, but it could suffer from the disparity in the quality of the distributions. The simplest way to address this issue would be to simply have more trials, which in turn would provide more data and a higher chance to better define the distributions for more clusters. It would also be beneficial in this situation to be able to remove the upper limit on datapoints to compare over, meaning running Monte Carlo simulations as in [24] for higher values of $n$.

Nevertheless, the results indicate there is a perceivable difference between using the robot-AR setup and performing the real-world equivalent task. The most likely cause would be that the damping and inertia of the robot were not low enough to properly convey full transparency during free motion. This could be the case, given the nature of the geared transmission system used in the robot and the admittance controller used to make it compliant. The implied difference in perceived weight during free motion would then be a likely cause in any changes in the observed biomechanics, as the user would compensate for the heavier load, experienced in the robot-AR condition, by adjusting their joint positions accordingly. In Fig. 4, this may be the reason why the E2S distributions have a much lower overall similarity than the H2E distributions, as the upper arm may have moved more in order to compensate for the larger resistance to motion in the robot-AR condition while the lower arm remained the same in order to hold the brush handle comfortably. There is then a motivation for reexamining the results when performed using a robot with similar load-bearing capabilities that is designed for the purpose of patient-safe interaction as well as built-in back-drivability (i.e., without internal gearing). Other robot designs such as those with series elastic actuators, or the use of variable impedance controllers is also worth exploring.

## V. Conclusion

In this paper, a robot-AR system that aims to be a suitable alternative to existing FCE and rehabilitation environments for injured or disabled workers is developed and evaluated. A task that involves painting a wall is presented to the participants. To evaluate our approach, the task has a real-life equivalent condition in which the biomechanics of the participant's arm for both robotic AR and real-life conditions are recorded and compared to determine if the arm movements are similar. Our results show that the arm biomechanics for a painting task have significant differences in $\approx 50\%$ of the collected clusters for the hand-to-elbow (H2E) displacements, and $\approx 30\%$ for the elbow-to-shoulder (E2S) displacements for both participants. These initial findings show the potential of our robot-AR system to replicate upper-limb movements found in traditional FCE and rehabilitation exercises and it motivates us to further investigate better methods to simulate functional tasks. Future work includes implementing the system with a different robot and/or robot controller that is better suited for physical human-robot interaction (PHRI), expanding the projected area, developing more tasks, and testing the system with actual FCE tasks, or even in a clinical setting. By creating an all-in-one robotic AR occupational rehabilitation system, we hope to motivate and provide an efficient method for workers to recover from their injuries.

## References


[1] D. P. Gross *et al.*, *Functional Capacity Evaluation*. New York, NY: Springer New York, 2017, pp. 1–4.

[2] BTE EvalTech. Https://www.btetech.com/product/evaltech/.

[3] Ergos II Work Simulator. http://www.simwork.com/Products/ErgosIIWorkSimulator.aspx.

[4] D. Peppers *et al.*, "Influence of functional capacity evaluation on physician's assessment of physical capacity of veterans with chronic pain: a retrospective analysis," *PM&R*, vol. 9, no. 7, pp. 652–659, 2017.

[5] D. P. Gross *et al.*, "A cluster randomized clinical trial comparing functional capacity evaluation and functional interviewing as components of occupational rehabilitation programs," *Journal of occupational rehabilitation*, vol. 24, no. 4, pp. 617–630, 2014.

[6] D. P. Gross *et al.*, "The prognostic value of functional capacity evaluation in patients with chronic low back pain: part 1: timely return to work," *Spine*, vol. 29, no. 8, pp. 914–919, 2004.

[7] F. Schaafsma *et al.*, "Physical conditioning programs for improving work outcomes in workers with back pain," *Cochrane Database Syst Rev*, vol. 1, 2010.

[8] C. James *et al.*, "Functional capacity evaluation research: Report from the second international functional capacity evaluation research meeting," *Journal of occupational rehabilitation*, vol. 26, no. 1, pp. 80–83, 2016.

[9] F. Yakub *et al.*, "Recent trends for practical rehabilitation robotics, current challenges and the future," *International Journal of Rehabilitation Research*, vol. 37, no. 1, pp. 9–21, 2014.

[10] B. Taylor *et al.*, "Workstation robotics: a pilot study of a desktop vocational assistant robot," *American Journal of Occupational Therapy*, vol. 47, no. 11, pp. 1009–1013, 1993.

[11] J. L. Schuyler *et al.*, "Assessing human-robotic performance for vocational placement," *IEEE Transactions on Rehabilitation Engineering*, vol. 8, no. 3, pp. 394–404, 2000.

[12] D. J. Reinkensmeyer *et al.*, ""If I can't do it once, why do it a hundred times?": Connecting volition to movement success in a virtual environment motivates people to exercise the arm after stroke," in *2007 Virtual Rehabilitation*, Sept 2007, pp. 44–48.

[13] H. M. Van der Loos *et al.*, "Rehabilitation and health care robotics," in *Springer handbook of robotics*. Springer, 2016, pp. 1685–1728.

[14] BTE Eccentron. Https://www.btetech.com/product/eccentron/.

[15] R. Ocampo *et al.*, "Improving user performance in haptics-based rehabilitation exercises by colocation of user's visual and motor axes via a three-dimensional augmented-reality display," *IEEE Robotics and Automation Letters*, vol. 4, no. 2, pp. 438–444, 2019.

[16] H. I. Krebs *et al.*, "Robot-aided neurorehabilitation," *IEEE transactions on rehabilitation engineering*, vol. 6, no. 1, pp. 75–87, 1998.

[17] J. Fong *et al.*, "Kinesthetic teaching of a therapist's behavior to a rehabilitation robot," in *2018 International Symposium on Medical Robotics (ISMR)*, March 2018, pp. 1–6.

[18] C. Martínez *et al.*, "Learning and robotic imitation of therapist's motion and force for post-disability rehabilitation," in *Systems, Man, and Cybernetics (SMC), 2017 IEEE International Conference on*. IEEE, 2017, pp. 2225–2230.

[19] N. Hogan *et al.*, "Impedance and interaction control," in *Robotics and automation handbook*, T. R. Kurfess, Ed. CRC press, 2004, ch. 19.

[20] F. Dimeas *et al.*, "Online stability in human-robot cooperation with admittance control," *IEEE Transactions on Haptics*, vol. 9, no. 2, pp. 267–278, April 2016.

[21] R. Tao, "Haptic teleoperation based rehabilitation systems for task-oriented therapy," Master's thesis, University of Alberta, 2015.

[22] Unity. Https://unity3d.com/.

[23] B. Jones *et al.*, "Roomalive: Magical experiences enabled by scalable, adaptive projector-camera units," in *Proceedings of the 27th Annual ACM Symposium on User Interface Software and Technology*, ser. UIST '14. New York, NY, USA: ACM, 2014, pp. 637–644.

[24] G. Fasano *et al.*, "A multidimensional version of the kolmogorov–smirnov test," *Monthly Notices of the Royal Astronomical Society*, vol. 225, no. 1, pp. 155–170, 1987.

[25] W. H. Press *et al.*, "Numerical recipes in c," *Cambridge University Press*, vol. 1, p. 3, 1988.